Chempublish Journal
Journal Homepage: online-journal.unja.ac.id/chp
Department of Chemistry
Faculty of Science and Technology
Universitas Jambi
ISSN (Online): ISSN 2503-4588
No. 23/E/KPT/2019

Article

Exploration of Belitung Taro Stems (*Xanthosoma sagittifolium*) as an Antidiabetic Candidate: An In Silico and In Vitro Approach

Wahyu Rahmatulloh, Sugeng Supriyanto*, Aditya Mahe Saputra, Nabila Aulia Rahma

[1]*Department pharmacy, Universitas Muhammadiyah Gombong, 54412 (Indonesia)*

Abstract

Diabetes mellitus is a global metabolic disorder characterized by chronic hyperglycemia. While conventional oral antidiabetics are effective, their long-term use is associated with adverse side effects, necessitating the search for safer alternatives from natural sources. Belitung taro (*Xanthosoma sagittifolium*) is a locally abundant tuber crop in Indonesia, but its stems are typically discarded as agricultural by-products despite their potential bioactive content. This study evaluated the antidiabetic potential of *X. sagittifolium* stem extract by investigating its α-amylase inhibitory activity through an integrative in silico and in vitro approach. In silico screening was performed on eight secondary metabolites from the CMAUP database, filtered based on Lipinski's Rule of Five and ADMET profiles using the pkCSM server. The lead compound, NPC141921, was docked into human pancreatic α-amylase (PDB ID: 2QV4) using AutoDock, validated by redocking acarbose. The ethanol extract was subjected to phytochemical screening and tested for α-amylase inhibition using the iodine-starch assay. NPC141921 showed a binding free energy of -6.13 kcal/mol, comparable to acarbose (-6.66 kcal/mol), forming stable hydrogen bonds with catalytic residues (ASP197, GLU233, ASP300) and substrate-binding residues (ARG195, HIS305). Phytochemical screening confirmed flavonoids, tannins, saponins, and steroids, supporting the *in silico* predictions. In vitro assays revealed an IC_{50} of 5028 ppm for the stem extract versus 1953 ppm for acarbose. Although the crude extract showed lower potency due to matrix dilution effects, the findings confirm that *X. sagittifolium* stems contain bioactive metabolites capable of α-amylase inhibition, highlighting their potential as a natural ingredient for hyperglycemia management.

Keywords: Diabetes Mellitus; *In silico*; *In vitro; Xanthosoma sagittifolium*

Graphical Abstract

* Corresponding author
Email addresses: sugengsupriyanto@unimugo.ac.id

DOI: https://doi.org/10.22437/chp.v10i1.48655
Received September 30th 2025; **Accepted** January 16th 2026; **Available online** May 18th 2026
Copyright © 2026 by Authors, Published by Chempublish Journal. This is an open access article under the CC BY License (https://creativecommons.org/licenses/by/4.0)

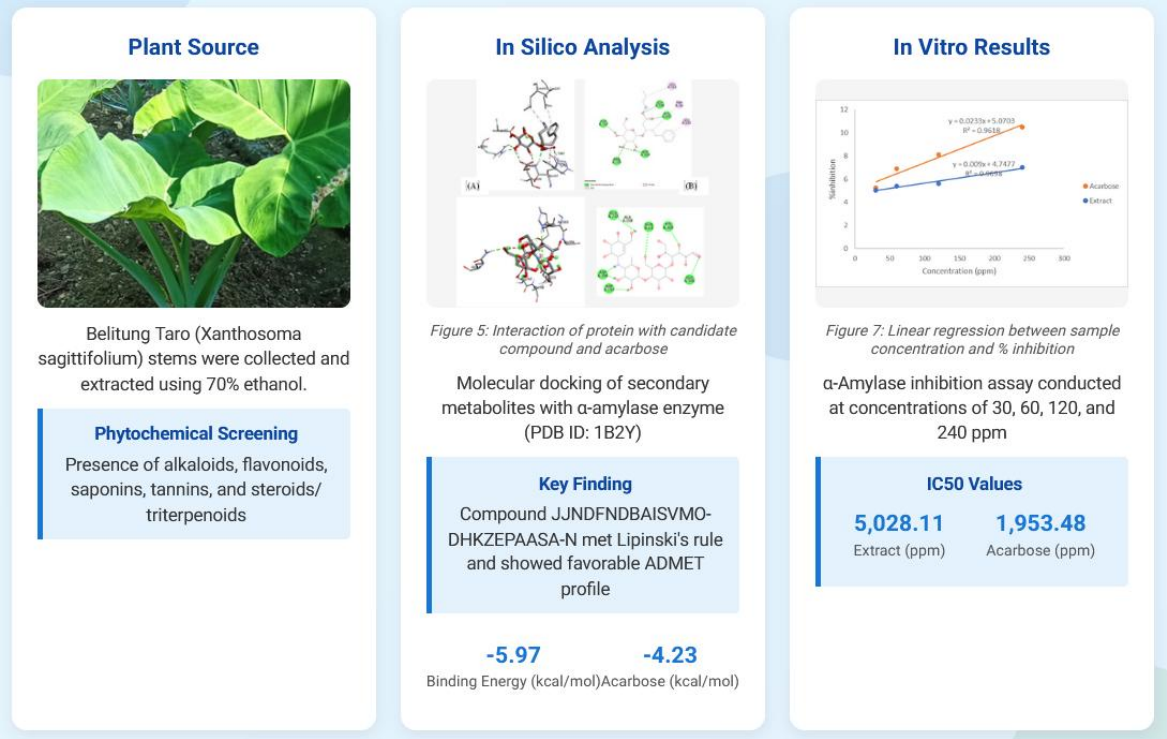

Introduction

Diabetes mellitus (DM) is a chronic disorder that occurs when insulin is not released in sufficient amounts or when insulin activity is ineffective due to metabolic resistance [1]. The International Diabetes Federation (IDF) reported a significant increase in global diabetes prevalence, with cases rising from 151 million to 537 million people worldwide, and the number projected to reach 783 million by 2045 [2]. The Indonesian Ministry of Health reported that Indonesia ranks fifth globally for the highest number of diabetes cases, with an estimated 21.3 million people affected by 2030 [3]. In the regional context, Kebumen Regency in Central Java, Indonesia, recorded approximately 12,000 diabetes cases in 2022, distributed across all its districts [4,5].

Although diabetes treatment with oral antidiabetic agents has advanced, the outcomes remain suboptimal. Several undesirable side effects have been reported with the use of metformin and sulfonylureas, such as diarrhea and lactic acidosis (metformin), as well as liver failure, weight gain, tachycardia, and hypothyroidism (sulfonylureas) [6,7]. In addition, issues such as drug resistance, adverse effects, and even toxicity have also been observed [8].

Belitung taro (*Xanthosoma sagittifolium*) is a traditional carbohydrate staple in Indonesia, with stems and tubers containing approximately 85% carbohydrate content (dry basis) and serving as a primary energy source for local populations. Belitung taro is traditionally consumed primarily for its carbohydrate-rich tubers, while the stems are typically discarded as agricultural by-products. Paradoxically, this high carbohydrate content provides the scientific rationale for antidiabetic investigation: as a widely consumed food source, any inherent α-amylase inhibitors within the plant could modulate postprandial glucose responses during consumption, offering a built-in glycemic control mechanism. However, previous studies have highlighted the species' broader medicinal potential,

including folk medicine applications for bone health, suggesting that non-edible parts may also contain bioactive compounds. The stems contain secondary metabolites including flavonoids, saponins, and tannins, compounds previously demonstrated to inhibit carbohydrate-metabolizing enzymes and improve insulin sensitivity in other plant species [9–13].

Scientific investigations into *Xanthosoma sagittifolium* have largely concentrated on the pharmacological properties of its leaves and tubers (corms). Previous studies have documented the antioxidant, antitumor, and iron-chelating activities of the leaf extracts. Additionally, the tubers have been evaluated for their nutritional value, calcium content for osteoporosis prevention, and potential as functional foods with low glycemic indices. However, the stems of *X. sagittifolium* remain an underutilized agricultural by-product with unexplored therapeutic potential. Unlike the tubers and leaves, scientific data specifically targeting the antidiabetic mechanisms of the stems is scarce. To date, there is a notable absence of studies integrating computational screening (*in silico*) with enzymatic assays (*in vitro*) to evaluate how secondary metabolites in the stems interact with key metabolic enzymes like α-amylase. This study aims to bridge this gap by repurposing the stems as a source of bioactive compounds for hyperglycemia management [14–17].

The combined in silico and in vitro approach consistently demonstrates effectiveness in mapping bioactive compound activity and validating their function in natural product research for antidiabetic purposes [18]. Molecular docking predicts compound interactions with target proteins such as α-amylase, while in vitro assays provide empirical evidence of enzyme inhibition and antihyperglycemic effects. This integrative method improves the efficiency of compound screening and strengthens the validity of research findings[18,19]. Therefore, this study aims to evaluate the effectiveness of compounds found in the stem of *Xanthosoma sagittifolium* as α-amylase inhibitors through *in silico* and *in vitro* assays.

Materials and Methods

Materials

The materials used include the three-dimensional structure of α-amylase protein (PDB ID: 2QV4) obtained from the Protein Data Bank, secondary metabolites of *Xanthosoma sagittifolium* stem retrieved from CMAUP using the keyword *Xanthosoma violaceum*, *Xanthosoma sagittifolium* stem, 96% ethanol, 2N HCl, distilled water, Mayer's reagent, Wagner's reagent, Dragendorff's reagent, 70% ethanol, magnesium powder, concentrated HCl, $FeCl_3$, chloroform, acetic anhydride, concentrated sulfuric acid, 100 mg acarbose, PBS (pH 7), α-amylase powder, starch powder, iodine, and potassium iodide.

Protein Receptor Preparation

The crystal structure of human pancreatic α-amylase (PDB ID: 2QV4) was retrieved from the RCSB Protein Data Bank (http://www.rcsb.org). This structure was selected for its high resolution of 1.97 Å and its co-crystallization with acarbose, providing the experimentally-defined binding pose essential for validating the docking protocol.. The protein was prepared using BIOVIA Discovery Studio Visualizer 2021, and saved in PDB format by removing water molecules, heteroatoms and the native acarbose ligand[20]. Polar hydrogen atoms were

subsequently added to ensure proper protonation states of amino acid residues. It was then separated from water (solvent), ligands, and non-standard residues.

Prediction of Pharmacokinetics, Toxicity, and Lipinski's Rule of Five

Prediction was conducted using the pkCSM platform http://structure.bioc.cam.ac.uk/pkcsm by entering the SMILES codes obtained from the CMAUP database[21]. The screening of bioactive candidates was performed in two sequential stages using the pkCSM web server (http://structure.bioc.cam.ac.uk/pkcsm) [22]. First, the drug-likeness of the compounds was assessed based on *Lipinski's Rule of Five* (Ro5). This rule predicts oral bioavailability by evaluating physicochemical parameters: molecular weight (≤ 500 Da), lipophilicity (LogP ≤ 5), hydrogen bond donors (≤ 5), and hydrogen bond acceptors (≤ 10) [23]. Compounds that failed to meet any single criterion of these rules were excluded from further analysis to strictly ensure optimal membrane permeability and oral bioavailability. Second, compounds passing the Ro5 filter were subjected to ADMET prediction using pkCSM's graph-based signature algorithms. This step evaluated pharmacokinetic parameters (e.g., intestinal absorption, volume of distribution, CYP450 inhibition) and toxicity endpoints (e.g., AMES mutagenicity, hepatotoxicity, LD50). The relationship between these two screenings is hierarchical: Lipinski's rule serves as a coarse filter for oral availability, while pkCSM provides a detailed safety and metabolic profile essential for selecting viable drug candidates [24,25]. ADMET predictions were assessed based on key pharmacokinetic indicators including intestinal absorption (>30%), predicted volume of distribution (log VDss between –0.15 and 0.45), cytochrome P450 inhibition (CYP2D6 and CYP3A4), total clearance, and toxicity endpoints [22]. Compounds were classified as *favorable* when they met these parameters, and *unfavorable* when they exceeded the thresholds or showed poor ADMET profiles.

Test Ligand Preparation

The test ligands were obtained from pharmacokinetic, toxicity, and Lipinski's rule predictions, and downloaded from PubChem by entering the smile code of the selected molecules, then saved in 3D conformer SDF format [14]. The ligands were subsequently optimized using the Avogadro application to minimize their energy and saved in PDB format [21].

Redocking (Validation)

AutoDock was used to re-dock the native ligand to the receptor protein, which generated grid box coordinates. These coordinates were then used both for redocking the native ligand (serving as the reference ligand) and for docking the secondary metabolites. Each redocking and docking run used 100 ligand conformations, a population size of 150, up to 2,500,000 energy evaluations, and 100,000 genetic generations, with all other parameters set to AutoDock defaults. The conformation with the lowest binding energy and an RMSD below 2 Å from the redocking served as a reference for subsequent docking of secondary metabolites from *Xanthosoma sagittifolium* [26].

Docking With Secondary Metabolites

AutoDock was used to dock the secondary metabolite compounds with the α-amylase protein, employing the same grid box settings as in the redocking/validation process to ensure consistency of results without significant variation between docking and redocking [26].

Interaction Study and Docking Result Visualization

The application used was BIOVIA Discovery Studio Visualizer 2021. The interactions between ligand and protein were visualized in both 2D and 3D, including van der Waals bonds, hydrophobic interactions, hydrogen bonds, and other interactions [27].

Data Analysis Technique

Data analysis included measurement of RMSD values and binding affinities from docking between the reference control and the test compounds. A T-test was then used to assess significant differences between them. An RMSD value of less than 2 Å indicates an accurate ligand position, while values greater than 2 Å suggest deviation [28]. Binding affinity measures the strength of interaction between a drug and its receptor; lower affinity values represent stronger binding, while higher values correspond to weaker binding [29].

Extract Preparation

The extract of *Xanthosoma sagittifolium* stem was prepared using the maceration method with 96% ethanol as the solvent. A total of 100 g of powdered simplicia was macerated at a ratio of 1:10 (w/v) for 3 × 24 h, with three repetitions. Maceration was carried out in a glass container placed in a location protected from direct sunlight, with occasional stirring. The obtained filtrate was separated from the simplicia and then concentrated using a rotary evaporator.

Phytochemical Screening

Alkaloid Screening: A total of 0.5 g of extract was added to 2 N HCl and 9 ml of distilled water, then heated for 2 min. After filtration, the filtrate was tested with Mayer's reagent (white or yellow precipitate indicates the presence of alkaloids), Dragendorff's reagent (orange color), and Wagner's reagent (brown color) [30]. ***Flavonoid Screening:*** the extract was mixed with 3 mL of 70% ethanol, shaken, heated, shaken again, and then filtered. The filtrate obtained was added with 0.1 g of magnesium powder and 2 drops of concentrated HCl. The formation of a red color in the ethanol layer indicated the presence of flavonoids [31]. ***Tannin Screening:*** A portion of the extract was placed into a test tube, added with hot water, and shaken until homogeneous for 5 min. Then, 3–4 drops of $FeCl_3$ were added. A greenish-blue (green-black) coloration indicated the presence of catechol tannins, while a bluish-black coloration indicated the presence of pyrogallol tannins [32]. *Saponin Screening*: A total of 0.5 g of extract was placed into a test tube. Then, 10 mL of hot water was added, and the mixture was cooled and shaken vigorously until homogeneous. The presence of saponins was indicated by the formation of a stable froth (1–3 cm height) that persisted for 30 seconds and did not disappear after the addition of one drop of 2 N hydrochloric acid [33]. ***Steroid and triterpenoid Screening****:* A total of 1 g of Xanthosoma sagittifolium stem extract was added with 20 drops of chloroform and then shaken until homogeneous. The filtrate obtained was subsequently added with 2 drops of acetic anhydride and 2 drops of concentrated sulfuric acid. A positive result is indicated by the appearance of a blue or green color for steroids, while a red or purple color indicates the presence of terpenoids [34].

α-Amylase Inhibitory Activity

The α-amylase inhibitory activity assay was conducted following the method described by Ononamadu et al. [34] with slight modifications. The α-amylase enzyme solution was prepared by dissolving 20 mg of α-amylase powder in 10 mL of phosphate buffer saline (PBS, pH 7). A 1% starch

solution was prepared by dissolving 250 mg of starch in 25 mL of distilled water under heating. The iodine solution was prepared by dissolving 16.6 mg of potassium iodide (KI) in a small volume of distilled water, followed by the addition of 25.4 mg of iodine (I_2), and then diluted to 20 mL with distilled water. A 1 N HCl solution was prepared by diluting 1.7 mL of concentrated HCl (37%) to 20 mL with distilled water. Acarbose standard solutions were prepared at concentrations of 30, 60, 120, and 240 ppm from a 1000 ppm stock solution obtained by dissolving 100 mg of acarbose in 100 mL distilled water. Similarly, the extract solution of *Xanthosoma sagittifolium* stems was prepared at the same concentrations from a 1000 ppm stock solution by dissolving 25 mg of extract in 25 mL distilled water and diluting accordingly.

The maximum wavelength (λmax) was determined by mixing 3000 µL of 1% starch solution with 200 µL of iodine solution, and the absorbance was scanned at 400–800 nm using a UV–Vis spectrophotometer. For the control, 2000 µL of phosphate-buffered saline (PBS) was incubated at 37 °C for 10 min, followed by the addition of 1000 µL of 1% starch solution and further incubation for 15 min. The reaction was terminated by adding 40 µL of HCl and 200 µL of iodine solution, and the absorbance was measured at λmax. For the sample treatment, 1000 µL of PBS was mixed with 1000 µL of α-amylase solution and incubated at 37 °C for 10 min prior to the addition of 1000 µL of 1% starch solution, followed by incubation for 15 min. The reaction was stopped using HCl and iodine solution, and the absorbance was subsequently measured at λmax.

For the sample control (KS), 1000 µL of extract or acarbose solution at each concentration was mixed with 1000 µL of PBS and incubated at 37 °C for 10 min, followed by the addition of 1000 µL of starch solution and further incubation for 15 min. The reaction was stopped with HCl and iodine solution before measuring the absorbance. For the sample (S), 1000 µL of extract or acarbose solution was mixed with 1000 µL of α-amylase solution and incubated at 37 °C for 10 min, followed by the addition of 1000 µL of starch solution and further incubation for 15 min. The reaction was terminated by adding HCl and iodine solution, and the absorbance was measured at λmax using a UV–Vis spectrophotometer. The inhibitory activity of α-amylase was expressed as the percentage of inhibition, which was calculated using the standard equation 1.

$$\% \text{ inhibition} = \frac{(K-U)-(KS-S)}{(K-U)} x100\% \quad (1)$$

Note:
K = Control absorbance
U = Enzyme control absorbance
KS = Sample control absorbance
S = Sample absorbance

To calculate IC_{50}, first plot sample concentration on the x-axis and % inhibition on the y-axis. Use the resulting linear regression equation to determine the concentration at which the percentage inhibition equals 50% (equation 2 - 4)

$$y = bx + a \quad (2)$$
$$50 = bx + a \quad (3)$$
$$x = \frac{(50-a)}{b} \quad (4)$$

Results and Discussion

Plant Determination

The plant determination was carried out at the Biology Laboratory, Universitas Ahmad Dahlan, Yogyakarta. The determination key is as follows: 1b – 2b – 3b – 4b – 12b – 13b – 14b – 17b – 18b – 19b – 20b – 21b – 22b – 23b – 24b – 25b – 26b – 27b – 799b – 800b – 801b – 802a – 803b – 804b – 805b Araceae

1b – 2b – 3b – 5b – 8a – 9a – 10a – 11b Xanthosoma

1 *Xanthosoma nigrum* (Vell.) Mansf.

Synonym of:

Xanthosoma atrovirens C. Koch & Bouché

Xanthosoma violaceum Schoot

Xanthosoma nigrum Stellfeld

Xanthosoma sagittifolium (L.) Schott

The plant material used in this study was taxonomically identified at the Biology Laboratory, Universitas Ahmad Dahlan. The specimen was determined as Xanthosoma sagittifolium (family Araceae), which is taxonomically synonymous with *Xanthosoma nigrum* (Vell.) Mansf. Identification was performed using a standard taxonomic identification key based on morphological characteristics, beginning from the family level (Araceae), followed by the genus *Xanthosoma*, and subsequently confirming the species as *X. sagittifolium* [35–37].

This synonymization is important. Several references mention *X. nigrum* (an alternate scientific name for X. sagittifolium) as a synonym of *X. sagittifolium. This strengthens* the validity of the plant material's taxonomic identification in this research. These determination results provide a strong and valid basis for developing antidiabetic phytopharmaca using Belitung Taro stems (*Xanthosoma sagittifolium*) [35–38].

In Silico Investigation

In this study, the selection of ligand compounds was performed using a *knowledge-based screening* approach utilizing the CMAUP (Collective Molecular Activities of Useful Plants) database. While direct metabolite profiling (e.g., via LC-MS) provides sample-specific data, database mining serves as a widely accepted preliminary strategy to predict potential bioactivity based on chemotaxonomic data. The eight metabolites selected (Table 1) were retrieved using the keyword *Xanthosoma violaceum* (a synonym for *X. sagittifolium*) and have been previously documented in the genus *Xanthosoma*. This approach allows for the screening of "likely" bioactive candidates to narrow down molecular targets before costly extraction and isolation procedures. Ideally, this *in silico* prediction serves as a hypothesis-generating step to guide future targeted isolation, rather than a confirmation of the extract's exact composition. To mitigate this limitation, standard qualitative phytochemical screening was performed in parallel (Section 3.3) to confirm the presence of major metabolite classes (alkaloids, flavonoids, tannins) predicted by the database[39–41]. Eight secondary metabolites were identified in the CMAUP database from Belitung taro stems using the keyword Xanthosoma violaceum (Table 1) [42].

All identified secondary metabolites were subsequently evaluated for their drug-likeness properties using Lipinski's Rule of Five (Table 2). According to Lipinski's criteria, a compound is considered to possess favorable oral bioavailability when it fulfills the following parameters: molecular weight (MW) < 500 Da, partition coefficient (log P) < 5, hydrogen bond donors (HBD) < 5, and hydrogen bond acceptors (HBA) < 10. Compounds that satisfy these criteria are generally predicted to exhibit good membrane permeability and absorption characteristics [1].

Table 1. Secondary Metabolites of Belitung Taro Stems (Source: CMAUP)

No.	NP_ID	Metabolite Name	Smiles Code	Structure
1.	NPC78263	Trifolin	c1cc(ccc1c1c(c(=O)c2c(cc(cc2o1)O)O)O[C@H]1[C@@H]([C@H]([C@H]([C@@H](CO)O1)O)O)O)O	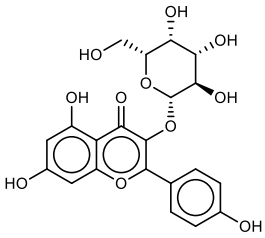
2.	NPC76315	(R)-5-phenyl-3-(((2R,3R,4S,5S,6R)-3,4,5-trihydroxy-6-(hydroxymethyl)tetrahydro-2H-pyran-2-yl)oxy)pentanoic acid	c1ccc(cc1)CC[C@H](CC(=O)O)O[C@H]1[C@@H]([C@H]([C@@H]([C@@H](CO)O1)O)O)O	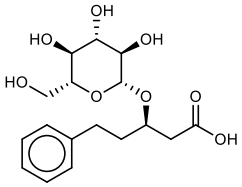
3.	NPC281131	Hyperoside	c1cc(c(cc1c1c(c(=O)c2c(cc(cc2o1)O)O)O[C@H]1[C@@H]([C@H]([C@H]([C@@H](CO)O1)O)O)O)O)O	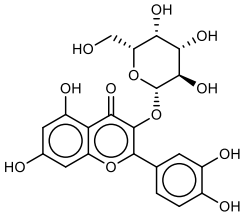
4.	NPC235260	Quercetin Glucuronide	c1cc(c(cc1c1c(c(=O)c2c(cc(cc2o1)O)O)O[C@H]1[C@@H]([C@H]([C@@H]([C@@H](C(=O)O)O1)O)O)O)O)O	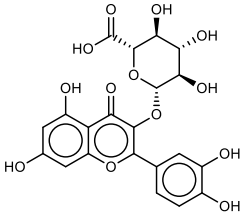
5.	NPC179950	Isoquercetin	c1cc(c(cc1c1c(c(=O)c2c(cc(cc2o1)O)O)O[C@H]1[C@@H]([C@H]([C@@H]([C@@H](CO)O1)O)O)O)O)O	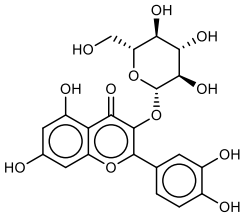
6.	NPC150546	1-(2-hydroxy-3,6-dimethoxy-4-(((2S,3R,4S,5S,6R)-3,4,5-trihydroxy-6-((((2R,3R,4S,5S,6R)-3,4,5-trihydroxy-6-(hydroxymethyl)tetrahydro-2H-pyran-2-yl)oxy)methyl)tetrahydro-2H-pyran-2-	COc1cc(c(c(c1C(=O)CCc1ccccc1)O)OC)O[C@H]1[C@@H]([C@H]([C@@H]([C@@H](CO[C@H]2[C@@H]([C@H]([C@@H]([C@@H](CO)O2)O)O)O)O1)O)O)O	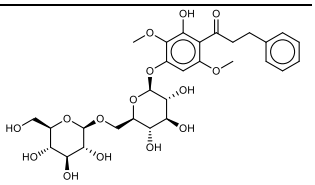

No.	NP_ID	Metabolite Name	Smiles Code	Structure
		yl)oxy)phenyl)-3-phenylpropan-1-one.		
7.	NPC141921	butyl (R)-5-phenyl-3-(((2R,3R,4S,5S,6R)-3,4,5-trihydroxy-6-(hydroxymethyl)tetrahydro-2H-pyran-2-yl)oxy)pentanoate	CCCCOC(=O)C[C@@H](CCc1ccccc1)O[C@H]1[C@@H]([C@H]([C@@H]([C@@H](CO)O1)O)O)O	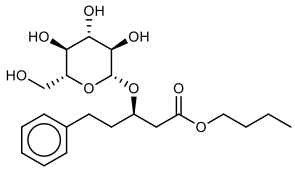
8.	NPC113836	Isoquercitin 2''-O-Gallate	c1cc(c(cc1c1c(c(=O)c2c(cc(cc2o1)O)O)O[C@H]1[C@@H]([C@H]([C@@H]([C@@H](CO)O1)O)O)OC(=O)c1cc(c(c(c1)O)O)O)O)O	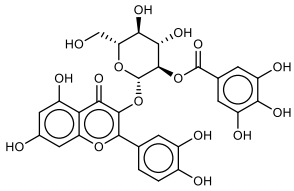

A molecular weight greater than 500 Da indicates that a compound is unlikely to penetrate the cell membrane; therefore, the molecular weight of secondary metabolites should be less than 500 Da. The higher the log P value, the more hydrophobic the molecule becomes. Excessively hydrophobic molecules tend to exhibit a higher level of toxicity. The number of hydrogen bond donors and acceptors describes the hydrogen bonding capacity, where an increased number corresponds to greater energy requirements for the absorption process to occur [2].

Table 2. Lipinski's Rule of Five Screening Results (Source: pkCSM)

Secondary Metabolites	Lipinski's Rule			
	BM (≤500)	HBD (≤5)	HBA (≤10)	Log P (≤5)
NPC78263	448.1	7.0	11.0	0.828
NPC76315	**356.15**	**5.0**	**8.0**	**-0.112**
NPC281131	464.1	8.0	12.0	0.462
NPC235260	478.07	8.0	13.0	0.688
NPC179950	464.1	8.0	12.0	0.225
NPC150546	626.608	8	15	-1.7722
NPC141921	412.21	4.0	8.0	1.866
NPC113836	616.11	10.0	16.0	1.297

Secondary metabolites that pass Lipinski's rule of five screening are those that meet all of its criteria. From the Lipinski screening of eight secondary metabolites, two compounds were found to satisfy the requirements, namely NPC76315 and NPC141921 (Table 2).

The compounds that passed the Lipinski's rule of five screening were subsequently subjected to pharmacokinetic and toxicity prediction to determine their pharmacokinetic profiles, including Absorption, Distribution, Metabolism, Excretion, and Toxicity (ADMET) (Table 3). The results of the pharmacokinetic and toxicity screening of the two secondary metabolites showed that only one compound met the requirements, namely NPC141921.

Based on pharmacokinetic and toxicity screening, the first parameter used was Absorption. The compound demonstrated good intestinal Absorption with an Intestinal Absorption value of 47.902%. A compound is considered to have good intestinal Absorption if its Intestinal Absorption value exceeds 30%. Intestinal Absorption is directly related to the ability of the intestine to absorb a drug administered orally [3].

The following pharmacokinetic prediction parameter is distribution. Distribution refers to the process by which a drug enters the systemic circulation. The greater the extent of distribution throughout the body, the faster the drug can reach its target site and exert its therapeutic effect. The distribution parameter assessed was VDss (volume of distribution at steady state). A compound is considered to have a low volume of distribution when the Log VDss value is < –0.15, and high when it is > 0.45. The volume of distribution (VDss) represents a theoretical volume required for the total administered dose of a drug to be uniformly distributed, achieving the same concentration as in plasma. A higher VD value indicates a greater proportion of the drug is distributed into tissues rather than remaining in the plasma [4].

The volume of distribution (VD) of acarbose is relatively low, approximately 0.32 L/kg, based on data from studies in healthy volunteers that calculated VD from plasma concentrations following intravenous administration. This low VD value indicates that acarbose is primarily retained in the plasma and gastrointestinal tract, with minimal distribution into tissues. This finding is consistent with the mechanism of action of acarbose, which mainly inhibits the α-glucosidase enzyme in the intestine rather than exerting effects in other tissues of the body [6,8,43].

The third pharmacokinetic parameter is metabolism. In general, metabolism occurs in the liver and is facilitated by cytochrome P450 enzymes. Cytochrome P450 (CYP) plays a crucial role in detoxification by oxidising xenobiotics for excretion. This enzyme family is responsible for the metabolism of many drugs, including CYP1A2, CYP2C9, CYP2D6, and CYP3A4/5, which together account for approximately 72% of overall drug metabolism [44]. Based on the results of metabolism screening, represented by the cytochrome isoforms CYP2D6 and CYP3A4, one compound was found not to inhibit the metabolism of CYP2D6 or CYP3A4. Therefore, the compound can be metabolised by these enzymes.

The final pharmacokinetic parameter is excretion. The excretion process of a compound can be assessed by measuring the Total Clearance (CLTOT) value. CLTOT represents the combination of hepatic clearance (metabolism in the liver and bile) and renal clearance (excretion via the kidneys) [4]. This parameter is closely related

to bioavailability and is critical for determining the appropriate dosage to achieve a steady-state concentration. The CLTOT value can be used to predict the rate of compound elimination. Based on the excretion screening results, the compound showed a CLTOT value of 1.438. Another important parameter is toxicity, which is evaluated through the LD_{50} value. LD_{50} is defined as the single dose of a test compound, calculated statistically, that causes the death of 50% of the test animals following oral administration [18].

The LD_{50} screening results showed that the compound had an LD_{50} value of 2.148 mol/kg. The compound that passed the pharmacokinetic and toxicity screening was then prepared for the next step, namely, molecular docking. The docking process began with validation, which involved separating the protein from its native ligand, followed by re-docking the separated protein and ligand. The validation stage began with protein preparation, which involved removing water molecules, native ligands, and other complex compounds contained within the structure [19,45]

The prepared protein was then used for validation through a redocking process with its native ligand. Prior to *redocking*, the native ligand was prepared by removing the protein and other associated complex molecules, leaving only the ligand. The results of the protein and native ligand preparation are presented in the figure 1.

Table 3. Pharmacokinetic and Toxicity Screening Results (Source: pkCSM)

Parameter	NPC76315	NPC141921
Intestinal Absorption (human) (% Absorbed)	21.616	47.902
VDss (human) (log L/kg)	-0.783	-0.636
CYP2D6 substrate	No	No
CYP3A4 substrate	No	No
CYP2D6 inhibitor	No	No
CYP3A4 inhibitor	No	No
Total clerance (log ml/min/kg)	1.247	1.438
LD_{50} (mol/kg)	2.311	2.148

The compound that passed the pharmacokinetic and toxicity screening was subsequently subjected to molecular docking analysis. This process began with a validation step, in which the protein was separated from its native ligand and then re-docked to ensure the accuracy of the docking method. Protein preparation was carried out by removing water molecules, the native ligand, and other complex molecules [6,8] Subsequently, the native ligand was also prepared by eliminating the protein and other associated molecules, leaving only the ligand, so that both were ready for the redocking stage.

The prepared protein and native ligand were subsequently validated by re-docking the ligand into the binding site of the separated protein. The validation results showed that the ligand successfully returned to its original position with high accuracy (Figure 1), as indicated by a Root Mean Square Deviation (RMSD) value of 1.51 Å. Validation is considered successful when the RMSD value is less than 2 Å [1]. An RMSD value closer to 0 indicates that the ligand can be precisely restored to its native binding pose.

Therefore, the validation process requires an RMSD value of < 2 Å to be deemed valid, ensuring that the docking protocol can be reliably applied for screening the candidate compounds [46].

To assess the accuracy of the docking protocol, the redocked acarbose conformation (blue) was superimposed onto the native crystallographic ligand (red) within the active site of 2QV4. As illustrated in Figure 1, the two conformations exhibited a high degree of overlap, particularly in the core hexasaccharide rings involved in catalytic interactions. The calculated RMSD of 1.51 Å confirms that the docking algorithm successfully reproduced the bioactive pose of the inhibitor with minimal deviation from the experimental structure. This structural alignment validates the grid box parameters and scoring function used for subsequent screening of candidate compounds [47].

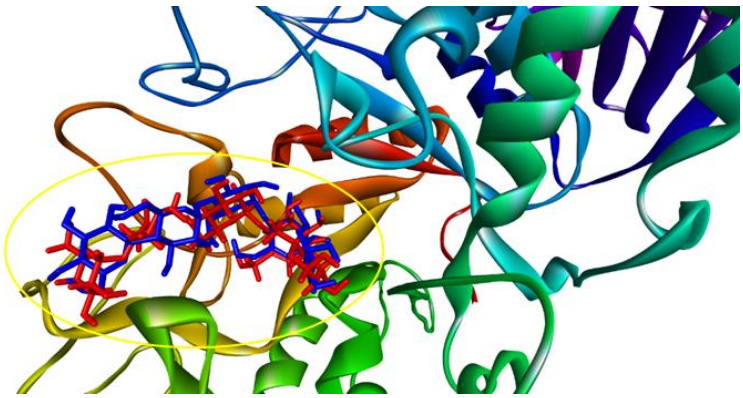

Figure 1. Validation Results. Native ligand (blue) and re-docked ligand (red)

The validation parameters were then used to perform the docking process with the candidate compounds. The parameter applied was the grid parameter file (GPF), obtained from the validation results, which contains information on the grid box size and grid box position (Table 4) [46]. The grid box size represents the dimensions of the grid box, while the grid box position describes the three-dimensional coordinates of the ligand in terms of X, Y, and Z points.

The candidate drug compound was first prepared prior to the docking process (Figure 4). Preparation was carried out by optimising the molecule through energy minimisation using Avogadro software. This step aimed to obtain a stable three-dimensional molecular structure [19]. The prepared candidate drug compound was then subjected to docking with the target protein.

Table 4. Validation Results of the Docking Process

Parameter	Value
Grid Box Size (Å)	44 x 40 x 40
Grid Box Position	X : 13.378
	Y : 47.46
	Z : 26.277
Spacing	0.375
RMSD	1.51 Å
Binding energy	-6.66 kcal/mol

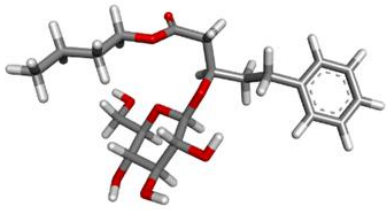

Figure 4. Optimized Candidate Drug Compound 3D view (NPC141921).

The molecular docking simulation aimed to evaluate the binding affinity and interaction modes of the selected secondary metabolite, NPC141921, within the active site of human pancreatic α-amylase (PDB ID: 2QV4). The docking results revealed that NPC141921 possesses a binding free energy of -6.13 kcal/mol. While this affinity is slightly lower than that of the standard inhibitor acarbose (-6.66 kcal/mol) (Table X), the difference is marginal (< 1.0 kcal/mol). According to thermodynamic principles, a more negative binding free energy (ΔG) correlates with a more stable ligand-receptor complex. Thus, although acarbose demonstrates a theoretically stronger interaction, the comparable binding energy of NPC1421 suggests it can still spontaneously and stably occupy the enzyme's active pocket, acting as a competitive inhibitor potentially capable of blocking substrate access to the catalytic site [14,16,48].

Table 5. The binding interactions between the active compounds, and α-amylase (2QV4)

Protein	Compound	Binding Energy (kcal/mol)	Protein Residue	Type of Interaction	3D Interaction and 2D Interaction
2QV4	Native Ligand (Acarbose)	-6.66	ALA106	Hydrogen Bond	**3D View** 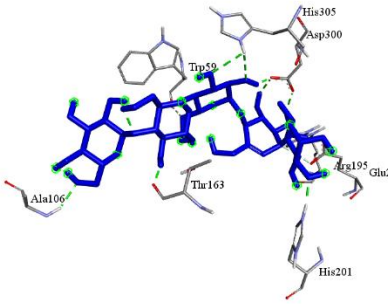
			ARG195	**Hydrogen Bond**	**2D View** 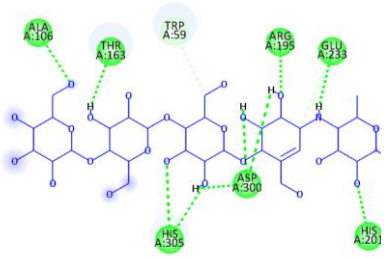
			ASP300	**Hydrogen Bond (3)**	
			GLU233	**Hydrogen Bond (2)**	
			HIS201	Hydrogen Bond	
			HIS305	**Hydrogen Bond (2)**	
			THR163	Hydrogen Bond	
			TRP59	**Hydrogen Bond**	

Protein	Compound	Binding Energy (kcal/mol)	Protein Residue	Type of Interaction	3D Interaction and 2D Interaction
	NPC141921	-6.13	GLN63	Hydrogen Bond (2)	**3D View** 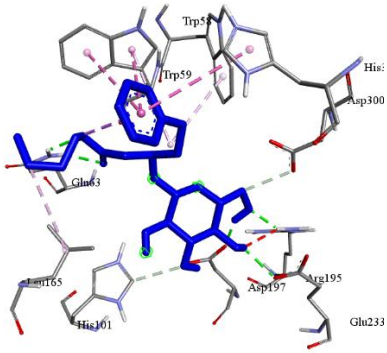
			ARG195	**Hydrogen Bond**	**2D View**
			ASP197	Hydrogen Bond (3)	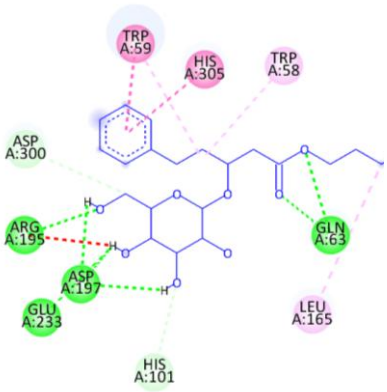
			GLU233	**Hydrogen Bond**	
			HIS101	Hydrogen Bond	
			ASP300	**Hydrogen Bond**	
			HIS305	**Hydrophobic**	
			TRP59	**Hydrophobic (3)**	
			LEU165	Hydrophobic	
			TRP58	Hydrophobic	

The catalytic site of human pancreatic α-amylase is mainly composed of three essential amino acid residues, namely ASP197, GLU233, and ASP300, which are directly involved in the hydrolysis of α-1,4-glycosidic linkages in starch substrates. ASP197 acts as the nucleophilic residue during catalysis, GLU233 functions as a proton donor and acceptor in the acid–base reaction mechanism, whereas ASP300 contributes to substrate orientation and stabilization of the transition state through hydrogen-bond interactions. Therefore, effective α-amylase inhibitors are generally

characterized by their ability to interact with one or more of these catalytic residues, thereby interfering with substrate binding and enzymatic activity [49–51].

Our analysis of the ligand-protein interactions revealed that NPC141921 forms hydrogen bonds with two of the three catalytic triad residues: ASP300 and GLU233 (Table 5). The formation of these hydrogen bonds is critical as it likely interferes with the proton transfer required for catalysis or stabilizes a non-productive conformation of the enzyme. Additionally, NPC141921 interacts with ARG195 and HIS305 via hydrogen bonds. Previous studies have highlighted that ARG195 and HIS305 are essential for substrate recognition and transition-state stabilization; inhibitors like acarbose are known to bind tightly to these residues to exert their inhibitory effect. The fact that NPC141921 shares these specific interaction partners (ARG195, GLU233, ASP300, HIS305 and TRP59) with the native ligand acarbose (Table 5) strongly supports a competitive inhibition mechanism [52,53]. It is well-established in rational drug design that the greater the similarity in key amino acid residues bound between a reference drug and a candidate compound, the higher the probability that the candidate will exhibit comparable biological activity [2,45].

Furthermore, NPC141921 exhibited hydrophobic interactions with TRP58, TRP59, and LEU165 within the active site cavity of α-amylase. Aromatic residues, particularly TRP59, are known to contribute to ligand stabilization through π–π stacking and hydrophobic interactions with carbohydrate-like moieties, thereby enhancing ligand binding stability. The simultaneous formation of hydrogen bonds with the catalytic residues and hydrophobic interactions within the binding pocket likely contributes to the strong binding affinity of NPC141921 toward α-amylase. These molecular docking results support the potential antidiabetic activity of Xanthosoma sagittifolium stem-derived compounds by suggesting their capability to inhibit α-amylase activity, which may subsequently delay carbohydrate hydrolysis and reduce postprandial glucose elevation [53].

Phytochemical Screening

Based on the research findings, it was confirmed that the stem extract of Belitung taro contains secondary metabolites, including alkaloids, flavonoids, steroids, saponins, and tannins. The results of the phytochemical screening of Belitung taro stem extract are presented in Table 6.

Phytochemical screening of Belitung taro stems (*Xanthosoma sagittifolium*) showed positive results for several secondary metabolites. The alkaloid test produced a white precipitate with Mayer's reagent, a brown precipitate with Wagner's reagent, and an orange colour with Dragendorff's reagent, indicating the presence of coordinate covalent bonds between alkaloid nitrogen and metal ions [20,27]. The flavonoid test using the Wilstater Cyanidin method showed a red colouration after the addition of Mg metal and concentrated HCl, confirming the presence of flavonoids [26]. The tannin test with $FeCl_3$ produced a bluish-green colour, indicating the formation of a tannin–$FeCl_3$ complex [29]. The saponin test showed positive results with the formation of stable foam due to the amphipathic structure of saponins forming micelles, particularly after the addition of HCl [26,27]. Finally, the steroid test showed a bluish-green colour after the addition of chloroform, acetic anhydride, and concentrated H_2SO_4, indicating the presence of steroids/triterpenoids through dehydration reactions and the formation of conjugated double bonds [31]

Table 6. Identification Results of the Extract Using Color Reagents

Compound Class	Reagent	Result	Note	Documentation
Alkaloids	Extract + 2N HCl + distilled water + Mayer's reagent	White precipitate	+	
	Extract + 2N HCl + distilled water + Wagner's reagent	Brown precipitate	+	
	Extract + 2N HCl + distilled water + Dragendorff's reagent	Orange color	+	
Flavonoids	Extract + 70% ethanol + Mg powder + concentrated HCl	Yellow color	+	
Tannins	Extract + 5% $FeCl_3$	Black color	+	
Saponins	Extract + hot water + 2N HCl	Foam formed & foam persists	+	

Compound Class	Reagent	Result	Note	Documentation
Steroids and Triterpenoids	Extract + acetic anhydride + concentrated H_2SO_4	Greenish-blue color	+	

In Vitro Antidiabetic Assay

Determination of Maximum Wavelength (λ max). This process is necessary because this stage has high sensitivity, so changes in absorbance at each concentration are the greatest and are measured within the wavelength range of 400–800 nm [34]. The maximum wavelength was obtained at 584 nm with an absorbance value of 1.0705. The results of the maximum wavelength determination are presented in Figure 6. Iodine solution is generally yellowish-brown in colour and will form a blue-colored complex when reacting with starch (amylose) [54]. Therefore, the absorbance measured by the UV-Vis spectrophotometer at the maximum wavelength of 584 nm indicates the amount of starch that is not hydrolysed by the enzyme.

α-Amylase Inhibition Assay. The α-amylase inhibition activity was evaluated using control, test, sample control, and sample solutions. The samples used in this study were the ethanol extract of Belitung taro stems and acarbose. Acarbose was used as a reference compound because it is an oral antidiabetic medication that inhibits glucose absorption in the intestine [55]. In principle, the more active the extract, the less starch is hydrolysed, resulting in lower glucose production, as the extract inhibits α-amylase activity. When the extract inhibits α-amylase, it cannot react with the starch substrate, producing a higher colour intensity [54,56]. The assay began by calculating the % inhibition for each concentration of the Belitung taro stem extract and acarbose. The concentrations tested were 30, 60, 120, and 240 ppm. The % inhibition value indicates the ability of the extract or acarbose at a specific concentration to inhibit α-amylase activity. The observed data for each concentration of the extract and acarbose are presented in Table 7.

Based on these results, the % inhibition values of the extract were very low at all tested concentrations, even at 240 ppm, where the inhibition did not exceed 11%. In contrast, acarbose showed a much higher percentage of inhibition at the same concentrations, consistent with its role as a standard α-amylase inhibitor. This difference is also reflected in the IC_{50} values, where the extract reached 5,028.111 ppm, significantly higher than that of acarbose at 1,953.478 ppm. A high IC_{50} value indicates that the extract has very weak inhibitory potential and requires a much higher concentration to achieve a meaningful effect. These findings suggest that the active compound content in the extract is likely low or insufficiently concentrated to produce a strong inhibitory effect.

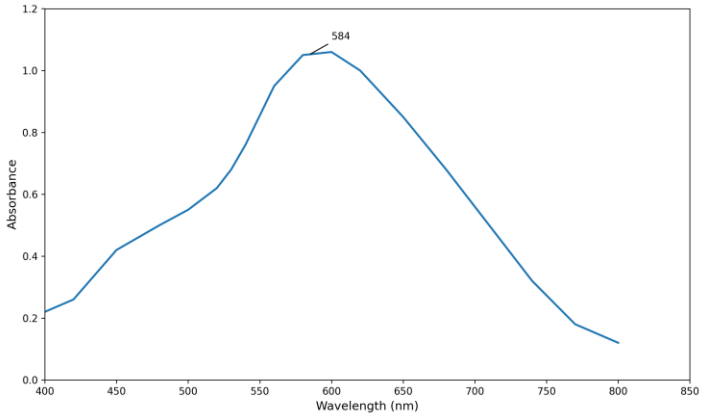

Figure 6. Results of Maximum Wavelength Determination

IC_{50} is the inhibitor concentration required to inhibit 50% of α-amylase enzyme activity [54]. The IC_{50} value can be determined using a linear regression equation, where the sample concentration is plotted on the x-axis and the % inhibition on the y-axis (Figure 7). Using the equation y=bx+ay = bx + ay=bx+a, the IC_{50} value can be calculated. The inhibitory activity of the *Xanthosoma sagittifolium* stem extract was quantified using a four-point concentration series (30–240 ppm), yielding an IC_{50} value of 5,028.11 ppm. While pharmaceutical method validation guidelines (e.g., ICH Q2) typically recommend a minimum of five to six concentration points for analytical assays, this study employed a streamlined four-point model suitable for preliminary bioactivity screening.

Table 6. Results of α-Amylase Inhibition by Belitung Taro Stem Extract and Acarbose

	% inhibition	
Concentration	**Extract**	**Acarbose**
30 ppm	5.05	5.248
60 ppm	5.399	6.912
120 ppm	5.616	8.121
240 ppm	6.996	10.499

The results of testing Belitung taro stem extract for α-amylase inhibitory activity showed an IC_{50} value of 5,028.111 ppm, with a correlation coefficient (r) of 0.984 and a linear regression equation of y = 0.009x + 4.7477. Meanwhile, acarbose, used as a control, exhibited an IC_{50} value of 1,953.478 ppm, with a correlation coefficient (r) of 0.980 and a linear regression equation of y = 0.0233x + 5.0703. The use of acarbose served to determine its IC_{50} as a positive control and to provide a comparison with the IC_{50} value of the tested extract.

Table 7. IC_{50} Values for α-Amylase Inhibition by the Extract and Acarbose

Sample	**IC_{50} (ppm)**
Extract	5,028.111
Acarbose	1,953.478

In our analysis, the linear regression models for both the extract and the acarbose standard demonstrated high linearity, with correlation coefficients (r) of 0.984 and 0.980, respectively. These values exceed the conventional acceptance threshold of r > 0.95 for exploratory biological assays, confirming that the four-point calibration curve provides a reliable and statistically valid estimation of potency for this investigative stage. Consequently, the calculated IC_{50} values serve as robust indicators of the extract's relative antidiabetic potential compared to the standard drug.

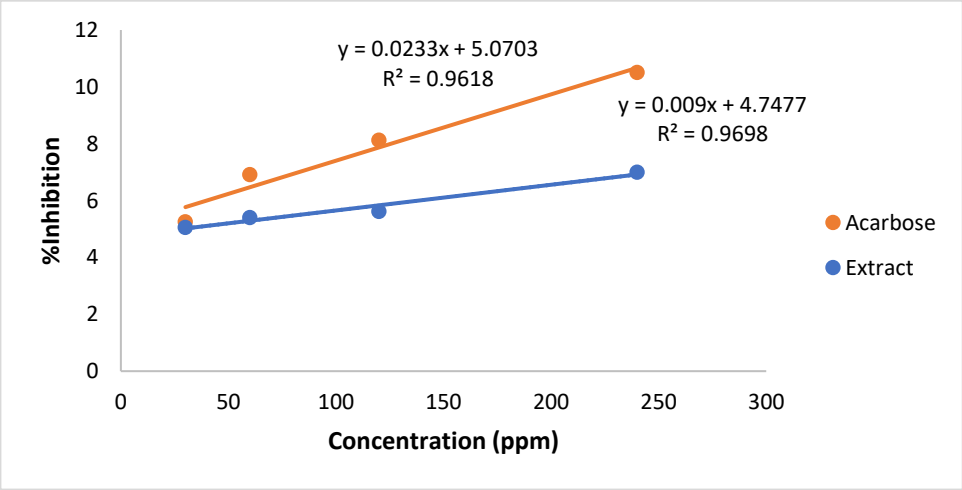

Figure 7. Linear regression between sample concentration and % inhibition of α-amylase

Based on the comparison between the Belitung taro stem extract and acarbose, it can be concluded that the ethanol extract of Belitung taro stems exhibits inhibitory activity against the α-amylase enzyme, thereby reducing its enzymatic action. The antidiabetic potential of this extract lies in its ability to inhibit α-amylase activity, which slows the conversion of complex carbohydrates into glucose, increases glycogen content in the liver, stimulates insulin secretion, and improves pancreatic beta-cell function [34]. However, the α-amylase inhibitory activity of acarbose remains more potent compared to the tested ethanol extract of Belitung taro stems.

Integrative Analysis of In Silico and In Vitro Findings

This study integrates computational predictions with experimental enzymatic assays to elucidate the antidiabetic potential of *X. sagittifolium* stems. A qualitative correlation was established between the two approaches: the *in silico* model identified flavonoid glycosides (e.g., NPC141921) as high-affinity ligands for α-amylase, which aligns with the phytochemical screening results confirming the presence of flavonoids in the extract. This suggests that the predicted bioactive ligands are likely constituents of the tested extract matrix [58].

Regarding the potency, the *in vitro* assay revealed that the crude stem extract exhibited an IC_{50} value of 5,028 ppm, which is higher than the standard acarbose (1,953 ppm). This difference in potency is characteristic of crude natural products, where the concentration of specific bioactive secondary metabolites is naturally diluted by non-active structural components such as cellulose and starch. Previous studies have consistently demonstrated that crude extracts display higher IC_{50} values comparedo their isolated pure compounds due to this matrix dilution effect. Consequently, while the docking results provide a mechanistic understanding of how specific flavonoids interact with the enzyme's active site, the *in vitro* results reflect the aggregate biological activity of the whole stem extract. These findings support the rationale for future bioassay-guided fractionation to isolate and validate the specific high-affinity compounds predicted by our computational model [14,16,17].

While *X. sagittifolium* tubers have been recognized for their nutritional value, the current findings demonstrate that the

stems—typically considered agricultural waste—possess significant α-amylase inhibitory activity. This expands the utility of the species beyond its conventional edible parts and aligns with reports of its broader ethnomedicinal applications [15,59].

Study Limitations and Future Directions.

The current *in silico* investigation focused on molecular docking to predict the binding affinity and interaction modes of the lead compound, NPC141921. While molecular docking provides a static snapshot of the ligand-receptor interaction, we acknowledge that it does not account for the flexibility and stability of the complex over time. Future studies incorporating Molecular Dynamics (MD) simulations will be valuable to assess the thermodynamic stability and conformational changes of the NPC141921-α-amylase complex in a solvated physiological environment, providing a more comprehensive understanding of its binding mechanism [60].

Furthermore, regarding the ligand selection, this study employed a hierarchical screening strategy where the eight initial metabolites were first filtered based on drug-likeness (Lipinski's Rule of Five) and ADMET safety profiles. Only NPC141921 satisfied all safety and pharmacokinetic criteria to justify its progression to the molecular docking stage. This funneling approach ensures that computational resources are focused on the most viable drug candidates with the highest probability of clinical translation, rather than screening compounds that would likely fail due to poor bioavailability or toxicity.

Conclusion

This study successfully evaluated the antidiabetic potential of Xanthosoma sagittifolium stems through an integrative in silico and in vitro approach. The computational screening identified NPC141921 as a promising lead compound, exhibiting a favorable ADMET profile and a strong binding affinity to human pancreatic α-amylase (PDB ID: 2QV4) with a binding energy of -6.13 kcal/mol. Molecular docking analysis revealed that NPC141921 interacts with key catalytic residues (ASP197, GLU233, ASP300) and substrate-binding residues (ARG195, HIS305) via hydrogen bonds, suggesting a competitive inhibition mechanism comparable to the standard drug acarbose. Experimentally, the ethanol extract of *X. sagittifolium* stems demonstrated α-amylase inhibitory activity with an IC_{50} value of 5,028 ppm. While this potency is lower than that of acarbose (1,953 ppm), likely due to the crude nature of the extract, the results confirm the presence of bioactive constituents capable of modulating carbohydrate metabolism. Collectively, these findings validate the traditional use of Belitung taro as a functional food resource and highlight the stem's potential as a raw material for developing natural antidiabetic agents. Further research focusing on the isolation of NPC141921 and in vivo efficacy studies is recommended to advance its pharmaceutical application.

Acknowledgement

This research was funded by the Ministry of Higher Education, Science, and Technology of the Republic of Indonesia under the 2024/2025 Beginner Lecturer Research (Penelitian Dosen Pemula) scheme.

Author Contributions

For research articles with several authors, a short paragraph specifying their individual contributions must be provided. The following statements should be used "Conceptualization, WR. and SS.; Methodology, WR. And SS.; Software, AM.;

Validation, WR., SS., AM and NA.; Formal Analysis, SS.; Investigation, WR and SS.; Data Curation, WR., SS., AM and NA; Writing – Original Draft Preparation, WR and SS.; Writing – Review & Editing, WR and SS; Visualization, WR and SS.; Supervision, WR and SS.; Project Administration, WR and SS.; Funding Acquisition, WR and SS.".

Conflict of Interest

The authors declare no conflict of interest.

References

[1] Nusantoro YR, Fadlan A. Analisis Sifat Mirip Obat, Prediksi ADMET, dan Penambatan Molekular Isatinil-2-Aminobenzoilhidrazon dan kompleks logam transisi Co(II), Ni(II), Cu(II), Zn(II) Terhadap BCL2-XL. *Akta Kimia Indonesia* 2020;5:114–26. https://doi.org/10.12962/j25493736.v5i2.7881.

[2] Naufa F, Mutiah R, Indrawijaya YYA. Studi in Silico Potensi Senyawa Katekin Teh Hijau (Camellia sinensis) sebagai Antivirus SARS CoV-2 terhadap Spike Glycoprotein (6LZG) dan Main Protease (5R7Y). JFood PharmSci 2022;10:584–96. https://doi.org/10.22146/jfps.3580.

[3] Inayah I, Aini FN, Hadisoebroto G. Studi In Silico Senyawa dari Herba Sambiloto (Andrographis paniculata) terhadap Protein Dihydrofolate Reductase (4KM2) pada Mycobacterium tuberculosis. Jurnal Sabdariffarma 2024;12:32–50. https://doi.org/10.53675/jsfar.v12i1.1317.

[4] Krihariyani D, Sasongkowati R, Haryanto E. Studi In Silico Sifat Farmakokinetik, Toksisitas, dan Aktivitas Imunomodulator Brazilein Kayu Secang Terhadap Enzim 3-Chymotrypsin-Like Cysteine Protease Coronavirus. Journal of Indonesian Medical Laboratory and Science 2020;1:76–90. https://doi.org/10.53699/joimedlabs.v1i1.1.

[5] Chaniad P, Mungthin M, Payaka A, Viriyavejakul P, Punsawad C. Antimalarial properties and molecular docking analysis of compounds from Dioscorea bulbifera L. as new antimalarial agent candidates. BMC Complement Med Ther 2021;21. https://doi.org/10.1186/s12906-021-03317-y.

[6] BPOM RI. Peraturan Badan Pengawas Obat dan Makanan Nomor 10 Tahun 2022 Tentang Pedoman Uji Toksisitas Praklinik Secara In Vivo. Indonesia: 2022.

[7] Shivanika, C., Deepak Kumar, S., Ragunathan, V., Tiwari, P., Sumitha, A., & Brindha Devi, P. (2022). Molecular docking, validation, dynamics simulations, and pharmacokinetic prediction of natural compounds against the SARS-CoV-2 main-protease. *Journal of Biomolecular Structure and Dynamics*, *40*(2), 585–611. https://doi.org/10.1080/07391102.2020.1815584

[8] Wada E, Feyissa T, Tesfaye K. Proximate, Mineral and Antinutrient Contents of Cocoyam (*Xanthosoma sagittifolium* (L.) Schott) from Ethiopia. *International Journal of Food Sciences,* 2019;2019:8965476. https://doi.org/10.1155/2019/8965476.

[9] Salehi B, Ata A, Kumar NVA, Sharopov F, Ramírez-Alarcón K, Ruiz-Ortega A, et al. Antidiabetic potential of medicinal plants and their active components. *Biomolecules* 2019;9:1–121. https://doi.org/10.3390/biom9100551.

[10] Kaur S, Gadpayale D, Kumari A, Kaur G, Kumar A, Seem K, et al. Antidiabetic potential of underutilized crops: Nutritional, phytochemical insights, and prospects for diabetes management. Applied Food Research 2025;5:101127. https://doi.org/10.1016/J.AFRES.2025.101127.

[11] Uti DE, Atangwho IJ, Alum EU, Egba SI, Ugwu OPC, Ikechukwu GC. Natural Antidiabetic Agents: Current Evidence and Development Pathways from Medicinal Plants to Clinical use. *Natural Product Communication*. 2025;20. https://doi.org/10.1177/1934578X251323393.

[12] Kustanti IH, Pudjirahaju A, Sulistiastutik, Puspita T. Subtitusi Pasta Talas Belitung (*Xanthosoma Sagittifolium* (L.) Schott), Tepung Tempe Kedelai Dan Tepung

Tapioka Dalam Pembuatan Mie Basah Untuk Penderita Diabetes Melitus. *Jurnal Agroteknologi*, 2013:129–42.

[13] Caxito MLC, Correia RR, Gomes ACC, Justo G, Coelho MGP, Sakuragui CM, et al. In Vitro Antileukemic Activity of *Xanthosoma sagittifolium* (Taioba) Leaf Extract. *Jurnal Evidence-Based Complementary and Alternative Medicine.* 2015;2015:384267. https://doi.org/10.1155/2015/384267.

[14] De Oliveira GL, De Holanda Cavalcanti Andrade L, Morais De Oliveira AF. Xanthosoma sagittifolium and Laportea aestuans: species used to prevent osteoporosis in Brazilian traditional medicine. *Pharmaceutical Biology* 2012;50:930–2. https://doi.org/10.3109/13880209.2011.637054.

[15] Nishanthini A, Mohan VR. Antioxidant activites of Xanthosoma sagittifolium Schott using various in vitro assay models. *Asian Pacific Journal of Tropical Biomedicine*, 2012;2:S1701–6. https://doi.org/10.1016/S2221-1691(12)60481-X.

[16] Handajani NS, Harini M, Yuliningsih R, Afianatuzzahra S, Hasanah U, Widiyani T. Assay for hypoglycemic functional food of cocoyam (Xanthosoma sagittifolium (L.) Schott.) tuber. *IOP Conference Series: Materials Science and Engineering* 2018;333:012074. https://doi.org/10.1088/1757-899X/333/1/012074.

[17] Nursamsiar, Mangande MM, Awaluddin A, Nur S, Asnawi A. In Silico Study of Aglycon Curculigoside A and Its Derivatives as α-Amilase Inhibitors. Indonesian Journal of Pharmaceutical Science and Technology Journal Homepage 2020;7:29–37. https://doi.org/10.24198/ijpst.v7i1.23062.

[18] Syahputra R, Utami D, Widyaningsih W. Studi Docking Molekuler Aktivitas Penghambatan Enzim Tirosinase Ubi Jalar (Ipomoea batatas L. Lam) Molecular Docking Study of Tyrosinase Enzyme Inhibition Activity of Sweet Potatoes (*Ipomoea batatas* L. Lam). *Pharmacon: Jurnal Farmasi Indonesia*. 2022;19:21–34. https://doi.org/10.23917/pharmacon.v19i1.18295.

[19] Ergina, Nuryanti S, Pursitasari D. Uji Kualitatif Senyawa Metabolit Sekunder Pada Daun Palado (Agave angustifolia) yang Diesktraksi Dengan Pelarut Air dan Metanol. *Jurnal Akademika Kimia*. 2014;3:165–72.

[20] Aziz Dwinuari R, Supriyanto S, Zukhruf Wakhidatul Kiromah N, Mahe Saputra A, Aji Pratama D. In Silico Study of the Potential of Belimbing Wuluh (Averrhoa bilimbi) for the Treatment of Type 2 Diabetes Mellitus. Chempublish Journal 2024;8:51–64. https://doi.org/10.22437/chp.v8i2.36624.

[21] Pires DEV, Blundell TL, Ascher DB. pkCSM: Predicting Small-Molecule Pharmacokinetic and Toxicity Properties Using Graph-Based Signatures. *Journal of Medicinal Chemistry*. 2015;58:4066–72. https://doi.org/10.1021/ACS.JMEDCHEM.5B00104.

[22] Lipinski CA, Lombardo F, Dominy BW, Feeney PJ. Experimental and computational approaches to estimate solubility and permeability in drug discovery and development settings. *Advanced Drug Delivery Reviews*. 1997;23:3–25. https://doi.org/10.1016/S0169-409X(96)00423-1.

[23] Ugbe FA, Shallangwa GA, Uzairu A, Abdulkadir I. Molecular Docking Investigation, Pharmacokinetic Analysis, and Molecular Dynamic Simulation of Some Benzoxaborole-Benzimidazole Hybrids: An Approach to Identifying Superior Onchocerca Inhibitors. Borneo Journal of Pharmacy 2023;6:58–78. https://doi.org/10.33084/BJOP.V6I1.3876.

[24] Muharrami LK, Santoso M, Fatmawati S. Chemical profiles, in silico pharmacokinetic and toxicity prediction of bioactive compounds from Boesenbergia rotunda. Case Studies in Chemical and Environmental Engineering 2024;10:100992. https://doi.org/10.1016/J.CSCEE.2024.100992.

[25] Muharrami LK, Santoso M, Fatmawati S. Chemical profiles, in silico

pharmacokinetic and toxicity prediction of bioactive compounds from Boesenbergia rotunda. *Case Studies in Chemical and Environmental Engineering*, 2024;10:100992. https://doi.org/10.1016/J.CSCEE.2024.100992.

[26] Haryati NA, Saleh C, Erwin. Uji Toksisitas Dan Aktivitas Antibakteri Ekstrak Daun Merah Tanaman Pucuk Merah (*Syzygium myrtifolium* Walp.) Terhadap Bakteri *Staphylococcus aureus* Dan Escherichia coli. *Jurnal Kimia Mulawarman* 2015;13.

[27] Salmia. Analisis Kadar Flavonoid Total Ekstrak Kulit Batang Kedondong Bangkok (*Spondias dulcis*) dengan Metode Spektrofotometro UV-VIS. *Universitas Islam Negeri Alauddin Makassar*, 2016.

[28] Halimu RB, Sulistijowati R, Mile L. Identifikasi Kandungan Tanin pada Sonneratia Alba. *Jurnal Ilmiah Perikanan dan Kelautan*, 2017;5:93–7. https://doi.org/10.37905/.v5i4.5291.

[29] Yuliyanti M, Husada VMS, Fahrudi HAA, Setyowati WAE. Quality and Detergency Optimization, Liquid Detergent Preparation, Mahogany Seed Extract (Swietenia mahagoni). *JKPK (Jurnal Kimia Dan Pendidikan Kimia)*, 2019;4:65–76. https://doi.org/10.20961/jkpk.v4i2.32750.

[30] Khafid A, Dwijunianto Wiraputra M, Christyaji Putra A, Khoirunnisa N, Awalia Kirana Putri A, Widodo Agung Suedy S, et al. Uji Kualitatif Metabolit Sekunder pada Beberapa Tanaman yang Berkhasiat sebagai Obat Tradisional. *Buletin Anatomi dan Fisiologi*, 2023;8:61–70. https://doi.org/doi.org/10.14710/baf.8.1.2023.61-70.

[31] Lallo S, Mirwan M, Palino A, Nursamsiar N, Hardianti B. Aktifitas Ekstrak Jahe Merah Dalam Menurunkan Asam Urat Pada Kelinci Serta Isolasi Dan Identifikasi Senyawa Bioaktifnya. *Jurnal Fitofarmaka Indonesia*, 2018;5:271–8. https://doi.org/10.33096/jffi.v5i1.319.

[32] A'yun Q, Laily AN. Analisis Fitokimia Daun Pepaya (*Carica papaya* L.) The Phytochemical Analysis of Papaya Leaf (Carica papaya L.) at The Research Center of Various Bean and Tuber Crops Kendalpayak, Malang. *Seminar Nasional Konversi dan Pemanfaatan Sumber Daya Alam,* 2015 2015:1341–137.

[33] Nurpatria MA, Muhtadi. Identifikasi Senyawa Kimia Dan Uji Aktivitas Inhibisi Enzim A-Amilase Ekstrak Etanol Akar Tembelekan (*Lantana Camara* L.). *Medical Sains : Jurnal Ilmiah Kefarmasian*, 2023;8:325–36. https://doi.org/10.37874/ms.v8i1.688.

[34] Ononamadu CJ, Ezeigwe OC, Owolarafe TA, Ihegboro GO, Lawal TA, Salawu K, et al. Starch-iodine assay method underestimates α-amylase inhibitory potential of antioxidative compounds and extracts. *Biotechnologia*, 2020;101:45–54. https://doi.org/10.5114/bta.2020.93103

[35] Jansen PCM, Premchand V. PROSEA - Plant Resources of South East Asia 1996. https://prosea.prota4u.org/view.aspx?id=3245 (accessed September 30, 2025).

[36] Fern K. Xanthosoma sagittifolium - Useful Tropical Plants 2014. https://tropical.theferns.info/viewtropical.php?id=Xanthosoma+sagittifolium&redir=Xanthosoma+nigrum (accessed September 30, 2025).

[37] Schott, H.W. Endlicher. S.L. *Xanthosoma sagittifolium* (L.) Schott 1832;19. https://powo.science.kew.org/taxon/urn:lsid:ipni.org:names:269329-2 (accessed September 30, 2025).

[38] Faisal M, Hossain AI, Rahman S, Jahan R, Rahmatullah M. A preliminary report on oral glucose tolerance and antinociceptive activity tests conducted with methanol extract of *Xanthosoma violaceum* aerial parts. *BMC Complementary and Alternative Medicine.* 2014;14. https://doi.org/10.1186/1472-6882-14-335.

[39] Zeng X, Zhang P, Wang Y, Qin C, Chen S, He W, et al. CMAUP: a database of collective molecular activities of useful plants. *Nucleic Acids Research.* 2018;47:D1118. https://doi.org/10.1093/NAR/GKY965.

[40] [40] Tessema FB, Asfaw TB, Tadesse MG, Gonfa YH, Bachheti RK. In Silico Studies as Support for Natural Products Research. Medinformatics 2025;2:11–21.

https://doi.org/10.47852/BONVIEWMEDIN42023842.

[41] Das AP, Agarwal SM. Recent advances in the area of plant-based anti-cancer drug discovery using computational approaches. *Molecular Diversity*. 2023;28:1. https://doi.org/10.1007/S11030-022-10590-7.

[42] Hou D, Lin H, Feng Y, Zhou K, Li X, Yang Y, et al. CMAUP database update 2024: extended functional and association information of useful plants for biomedical research. *Nucleic Acids Research.* 2024;52:D1508–18. https://doi.org/10.1093/nar/gkad921.

[43] BPOM. Peraturan Kepala Badan Pengawas Obat dan Makanan Republik Indonesia Nomor 7 Tahun 2014 Tentang Pedoman Uji Toksisitas Nonklinik Secara In Vivo. Indonesia: 2014.

[44] Frimayanti N, Lukman A, Nathania L. Studi molecular docking senyawa 1,5-benzothiazepine sebagai inhibitor dengue DEN-2 NS2B/NS3 serine protease. *Chempublish Journal* 2021;6:54–62. https://doi.org/10.22437/chp.v6i1.12980.

[45] Klara IK, Purwono RM, Achmadi P. Analisis In Silico Senyawa Flavonoid Kayu Secang (*Caesalpinia sappan* L.) pada Reseptor α-Amilase Sebagai Antihiperglikemik. *Acta Veterinari Indonesiana,* 2023;11:210–9. https://doi.org/10.29244/avi.11.3.210-219.

[46] Pratama MRF, Poerwono H, Siswodihardjo S. Introducing a two-dimensional graph of docking score difference vs. similarity of ligand-receptor interactions. *Indonesia Journal of Biotechnology.* 2021;26:54–60. https://doi.org/10.22146/IJBIOTECH.62194.

[47] Rao SN, Head MS, Kulkarni A, LaLonde JM. Validation Studies of the Site-Directed Docking Program LibDock. *Journal of Chemical Information and Modeling*. 2007; 47:2159–71. https://doi.org/10.1021/CI6004299.

[48] De Almeida Jackix E, Monteiro EB, Raposo HF, Amaya-Farfán J. Cholesterol reducing and bile-acid binding properties of taioba (Xanthosoma sagittifolium) leaf in rats fed a high-fat diet. *Food Research International* 2013;51:886–91. https://doi.org/10.1016/J.FOODRES.2013.02.017.

[49] Neves RPP, Fernandes PA, Ramos MJ. Role of Enzyme and Active Site Conformational Dynamics in the Catalysis by α-Amylase Explored with QM/MM Molecular Dynamics. *Journal of Chemical Information and Modeling*. 2022;62:3638. https://doi.org/10.1021/ACS.JCIM.2C00691.

[50] Basnet S, Ghimire MP, Lamichhane TR, Adhikari R, Adhikari A. Identification of potential human pancreatic α-amylase inhibitors from natural products by molecular docking, MM/GBSA calculations, MD simulations, and ADMET analysis. *BioRxiv*, 2022:2022.09.26.509544. https://doi.org/10.1101/2022.09.26.509544.

[51] Singh R, Sindhu J, Singh D, Kumar P. Key molecular scaffolds in the development of clinically viable α-amylase inhibitors. *Future Medicinal Chemistry,* 2025;17:347–62.https://doi.org/10.1080/17568919.2025.2453421.

[52] Dalli M, Daoudi NE, Abrigach F, Azizi SE, Bnouham M, Kim B, et al. In vitro α-amylase and hemoglobin glycation inhibitory potential of Nigella sativa essential oil, and molecular docking studies of its principal components. *Frontiers in Pharmacology*. 2022; 13: 1036129.https://doi.org/10.3389/FPHAR.2022.1036129.

[53] Lolok N, Ramadhan DSF, Sumiwi SA, Sahidin I, Levita J. Molecular Docking Of β-Sitosterol And Stigmasterol Isolated From Morinda Citrifolia With α-Amylase, α-Glucosidase, Dipeptidylpeptidase-Iv, And Peroxisome Proliferator-Activated Receptor-γ. *Rasayan Journal of Chemistry* 2022;15:20–30. https://doi.org/10.31788/RJC.2022.1516646.

[54] Wirasti, Lestari T, Isty'aroh. Penghambatan Ekstrak Daun Kremah (Alternanthera sessilis) Terhadap Enzim α-amilase secara In-Vitro. *Pharmacon : Jurnal Farmasi Indonesia,* 2021;18:68–74. https://doi.org/10.23917/pharmacon.v18i01.14657.

[55] Hidayah N, Pratama KJ, Raharjo D. Aktivitas Penghambatan Enzim Alfa-Amilase Ekstrak Dan Fraksidaun Nipah (*Nypa Fruticans* Wurmb). *Jurnal Ilmiah Wahana Pendidikan,* Desember 2023;2023:677–84. https://doi.org/10.5281/zenodo.10433927

[56] Nasir A, Khan M, Rehman Z, Khalil AAK, Farman S, Begum N, et al. Evaluation of alpha-amylase inhibitory, antioxidant, and antimicrobial potential and phytochemical contents of polygonum hydropiper L. *Plants* 2020;9:1–13. https://doi.org/10.3390/plants9070852.

[57] Turner RJ., & Charlton SJ. Assessing the Minimum Number of Data Points Required for Accurate IC 50 Determination. *ASSAY and Drug Development Technologies*. 2005. 3(5), 525–531. https://doi.org/10.1089/adt.2005.3.525.

[58] Miranda CTCdS., Soares SD., de Oliveira WQ, Lima AdS, Neri Numa IA, Pastore GM. Unconventional Edible Plants of the Amazon: Bioactive Compounds, Health Benefits, Challenges, and Future Trends. *Foods*. 2024; 13(18):2925. https://doi.org/10.3390/foods13182925

[59] Mba CJ, Agu HO. Developments on the Bioactive Compounds and Food Uses of the Tubers: Colocasia esculenta (L) Schott (Taro) and *Xanthosoma sagittifolium* (L) Schott (Tannia). *Asian Food Science Journal* 2021;20:101–12. https://doi.org/10.9734/AFSJ/2021/V20I1130380.

[60] Sanik L, Fadil Amrulloh W, Harmastuti N, Prasetiyo A, Herowati R. Analysis of Molecular Docking and Dynamics Simulation of Mahogany (Swietenia macrophylla King) Compounds Against the PLpro Enzyme SARS-COV-2. *Jurnal Farmasi dan Ilmu Kefarmasian Indonesia* 2023;10:347–59. https://doi.org/10.20473/JFIKI.V10I32023.347-359.